Paper No. 1749. (quote when citing this article)
Eleventh World Conference on Earthquake Engineering
ISBN: 0 08 042822 3

Study on Hysteresis Behaviors of Precast Member Subassemblages Composed of High- and Normal-Strength Concrete

K. HAYASHI and A. MIKAME

Technical Research Institute, Fujita Corporation,
74, Ohdana-cho, Tsuzuki-ku, Yokohama 224, Japan

ABSTRACT

In this paper, two experimental studies regarding the use of different strengths of concrete together in reinforced concrete frame are described. The first study examines the hysteresis behaviors of reinforced concrete beams in which the precast portion and the cast-in-place portion are made of high-strength and normal-strength concrete, respectively. The other study concerns the shear behavior of interior beam-column subassemblages with additional steel plates on the rebar and additional reinforcement in the joint. From the experimental tests, a design method for ultimate beam shear strength is proposed. And, the ductility and shear bearing capacity of joint can be raised by using additional reinforcement.

KEYWORDS

Reinforced concrete; concrete strength; precast; beam; beam-column joint; ultimate strength.

INTRODUCTION

In recent years, the construction of high-rise buildings, has entailed a demand for increased span length and the reduction of members' cross-section. High-strength materials have been introduced to meet to these needs. However, the use of high-strength concrete, requires considerable work time and makes quality control difficult. These problems are of great concern to construction management. Consequently, with the aim of eliminating the existing workability disadvantages of high-strength concrete at construction sites, frames composed of high-strength concrete precast members and cast-in-place portions using normal-strength concrete have been developed.

This paper reports the result of experimental study on (a) the maximum shear strength of beams made of concrete with different strengths, and (b) improving the shear-resistance mechanism of beam-column subassemblages by adding reinforcement of panels.

SHEAR TEST OF BEAMS

Outline of Experiment

Four reinforced concrete beam specimens were tested under repeated cyclic earthquake-type loading. Their cross-sectional properties and overall configurations are shown in Table 1 and Fig. 1. Two specimens were constructed as rectangular sections (BNo.1 and 2), and the other two were constructed as T-shape sections (BNo.3 and 4). The specimens were 1/4-scale models with shear span to depth ratios of 1.67. They were designed to develop shear failure just before attaining critical bending strength. In specimens BNo.1 and 3, concrete with the same specified design strength as the precast portions was used for the cast-in-place portions (Fc=59MPa). In contrast, in specimens BNo.2 and 4, concrete of Fc=59MPa was used in precast portions, but concrete of Fc=29MPa was used in cast-in-place portions. The cast-in-place portions were the upper part of beam and floor slabs. The cast-in-place area in each specimen was twenty percent of the rectangular cross section. The mechanical properties of materials are shown in Table 2 and 3. High strength reinforcement of $\sigma_y \fallingdotseq 755$MPa and normal strength reinforcement of σ_y=422MPa were used as main rebar and shear reinforcement, respectively.

Table 1. Designated cross-sectional properties of beam specimens

Specimen	Slab thickness × width Floor rebar	Concrete strength of cast-in-place portion	Common properties
BNo.1	Not applicable	59 MPa	Beam width × depth = 200 mm × 300 mm, Clear span : 1000 mm, Concrete strength in precast portion : 59 MPa, Beam main rebar ratio pt=1.75%, Stirrup ratio pw=0.8%
BNo.2		29 MPa	
BNo.3	60 mm × 120 mm D6@60 (both longitudinal and lateral)	59 MPa	
BNo.4		29 MPa	

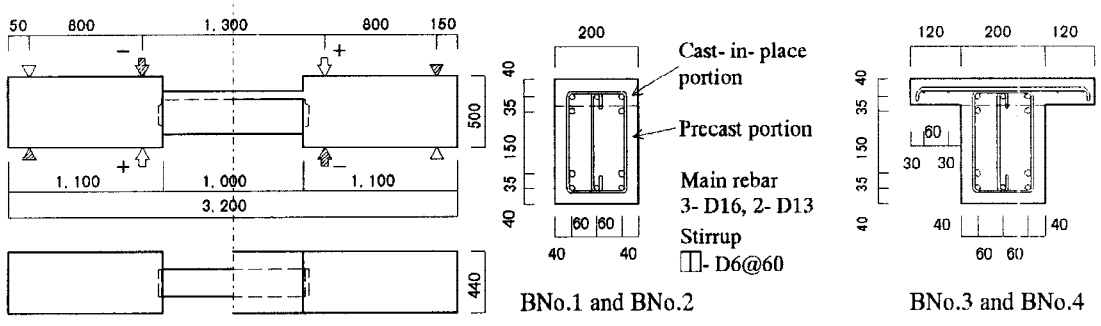

Fig. 1. Beam specimens

Table 2. Mechanical properties of rebars

Type	Yield point σ_y	Ultimate tensile strength σ_u	Young's modulus of elasticity E	Object
D6	422.8 MPa	551.6 MPa	1.794×10^5 MPa	Stirrup, Slab rebar
D13	757.7 MPa	970.0 MPa	2.029×10^5 MPa	Main rebar
D16	760.0 MPa	987.7 MPa	1.980×10^5 MPa	Main rebar

Table 3. Mechanical properties of concrete

Casting zone		Compressive strength σ_B	Young's modulus of elasticity E*	Split tensile strength σ_t
Precast portion		71.7 MPa	3.67 $\times 10^4$ MPa	3.82 MPa
Cast-in-place	BNo.1, 3	64.7 MPa	3.68 $\times 10^4$ MPa	3.10 MPa
	BNo.2, .4	30.3 MPa	2.60 $\times 10^4$ MPa	2.73 MPa

E* : measured at 1/4th of σ_B

Table 4. Principal measured values, and comparison with calculated values

		Initial stiffness		Strength at rebar yielding			Strength at maximum load			
	+ / -	exp.Ki	exp.Ki /cKi	exp.Qiy	exp.Qiy /cQiy	exp.Riy	exp.Qm	exp.Qm /c1Qm	exp.Qm /c2Qm	exp.Rm
JNo.1	+	1314	0.37	267	1.02	14.61	269	0.97	1.08	20.66
	-	-	-	-	-	-	261	0.94	1.05	20.31
JNo.2	+	2471	0.76	250	1.07	14.37	260	0.94	1.08	19.24
	-	-	-	-	-	-	247	0.89	1.02	18.25
JNo.3	+	2030	0.45	290	1.00	14.62	293	0.99	1.17	20.36
	-	-	-	282	1.01	16.28	289	0.98	1.15	20.06
JNo.4	+	2402	0.59	269	0.98	14.16	282	0.95	1.19	20.32
	-	-	-	261	0.90	19.54	261	0.88	1.10	19.54

Note : cKi: calculated elastic stiffness, cQiy: calculated by e-function method, c1Qm: calculated by approximate equation of Architectural Institute of Japan (AIJ), c2Qm: calculated by A-method equation of design guideline based on ultimate strength concept of AIJ. Unit : K [kN/cm], Q [kN], R [$\times 10^{-3}$rad.].

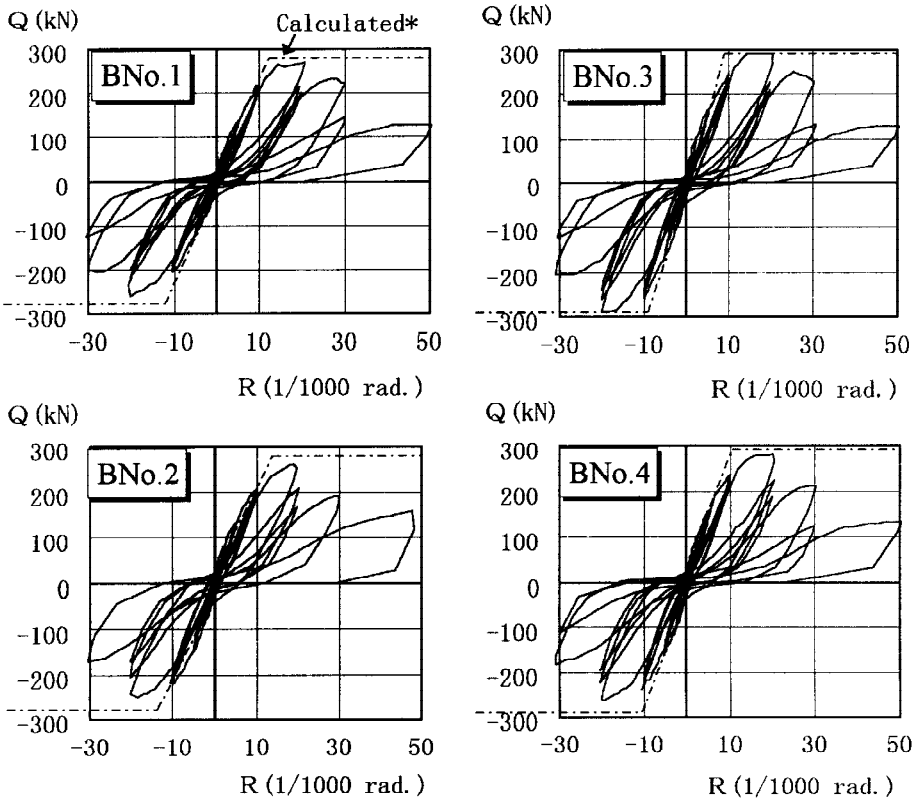

* : Calculated ultimate bending strength and yield point stiffness are based on approximate equation of AIJ and Sugano's equation, respectively.

Fig. 2. Hysteresis loops of shear force versus beam deformation angle

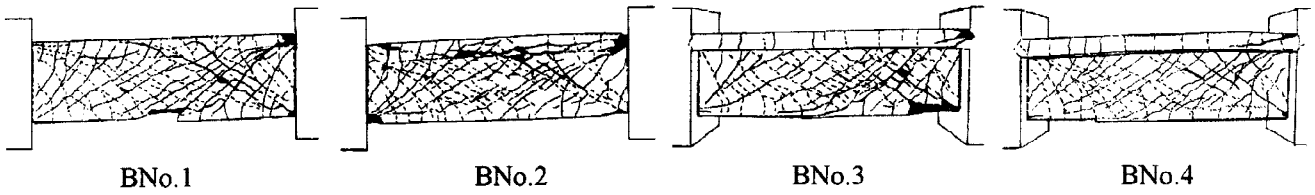

Fig. 3 Cracking patterns (at $R=30\times10^{-3}$rad.)

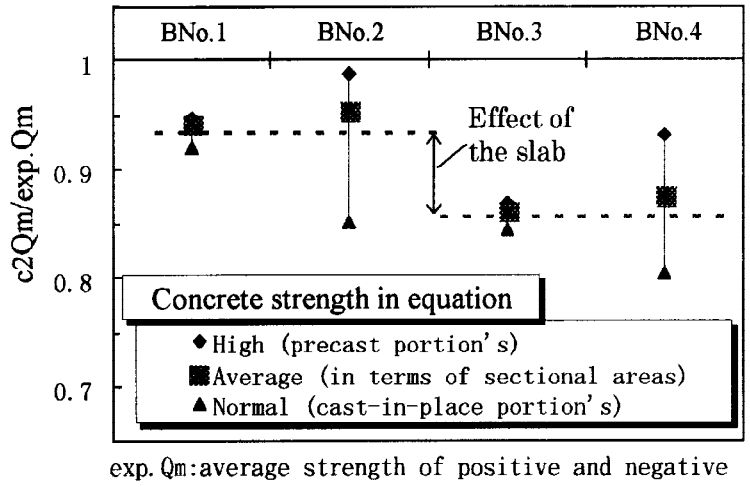

Fig. 4 Comparison of measured value and calculated value of ultimate shear strength

Experimental Results

Table 4 tabulates the principal measured values and comparison with calculated values, Fig. 2 shows the hysteresis loops of shear force versus beam deformation angle, and Fig. 3 depicts the cracking patterns at beam deformation angle $R=30\times10^{-3}$ *rad.* The initial stiffness for all test structures appeared lower than the calculated values. This trend was lower for the specimen with cast-in-place high-strength concrete in comparison to the specimen with cast-in-place normal-strength concrete. This seems to be due to the greater shrinkage effect of the high strength concrete at the precast joint of the beam end in comparison to the normal strength concrete. In all specimens, shear failure was observed immediately after yielding of longitudinal beam reinforcement. The locations of failure after reaching maximum strength tended to be concentrated in the region of normal-strength concrete. However, for all specimens, the difference in maximum strength of specimens using high-strength concrete for all portions and the specimens using normal concrete for cast-in-place portions was small. All specimens suffered beam yielding at $Rt\fallingdotseq15\times10^{-3}$ *rad* and attained maximum strength. At this stage, the deformation angle was $R=20\times10^{-3}$ *rad*, thereafter, the strength decreased abruptly. There was no distinguishable difference in the shear strength versus deformation angle hysteresis loops.

Shear Strength Fig. 4 shows the comparison between measured values of maximum strength (exp.Qm) and calculated values of shear strength (c2Qm.). The calculations were done according to the concrete strength concern from Comité Euro-International du Béton (CEB) Code and the A-method equation of design guidelines based on the ultimate strength concept of Architectural Institute of Japan (AIJ). The calculated shear strength values of specimens BNo.2 and 4 (made of different strength concrete) using normal strength of concrete were much lower than the measured values. But, the shear strength values of those specimens were similar to the specimens with conventional uniform-strength concrete (BNo.1 and 3) when estimated by using average strength in terms of sectional areas. The maximum strength of the specimen with slab was 10% higher than the specimen without slab, indicating the effectiveness of the slab. Also, even if the concrete strength of the cast-in-place portion was lower than that of the precast portion, the introduction of a

slab increased the shear strength to the same level as that of the rectangular section in which all portions were made of high-strength concrete.

EXPERIMENT ON BEAM-COLUMN SUBASSEMBLAGES

Outline of Experiment

Three 1/2-scale model specimens of beam-column subassemblages were tested. In specimen JNo.1, high-strength concrete of Fc=59MPa was used both in precast as well as cast-in-place portions. In the other two specimens, JNo.2 and 3, normal-strength concrete of Fc=29MPa was used in joint panels and cast-in-place portions of the upper part of the beam. Table 5 and Fig. 5 show the cross-sectional properties with reinforcement details. In designing the JNo.1 specimen, shear failure was assumed to occur after beam yielding at joint panels. In specimens JNo.2 and 3, the arrangement of beam reinforcement at locations other than joint panels and surrounding zones were the same as that of JNo.1. The shear stress level of the joints in specimens

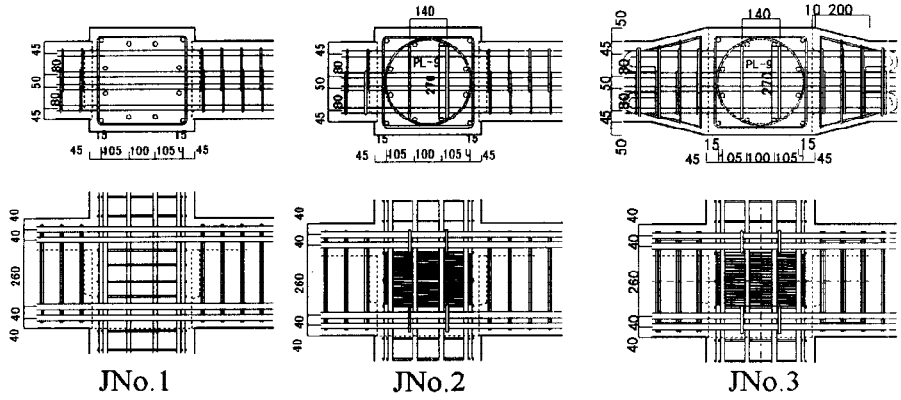

Fig. 5. Details of Joint Panels

Table 5. Designateed cross-sectional properties of beam-column joint specimens

Specimen	Concrete strength of joint panel	Anchor plate	Reinforcement of joint	Horizontal haunch
JNo.1	Fc59	None	□-D6@75	None
JNo.2	Fc29	$^{w}270\times^{H}80\times^{t}9$	□-D6@100 +	
JNo.3		×2peaces	○-U7.4@11	Add
Common properties	Span×Height = 3000×2000, Strength of concrete of precast portion : Fc=59MPa, Beam : Width×Depth=300×420, Main rebar :4-D19+2-D16, Stirrup : ▥-D6@75 Column :Width×Depth=400×400, Main rebar :12-D16, Hoop : ▣-D6@75			

Table 6. Mechanical properties of rebars

Type	Yield point σ_y	Ultimate tensile strength σ_u	Young's modulus E	Object
U6	820.5 MPa	1008.1 MPa	1.780×10^5 MPa	Spiral reinforcement of joint
U7.4	1373.9MPa	1464.1MPa	1.876×10^5 MPa	Hoop, Stirrup
D10	360.6MPa	491.3MPa	1.753×10^5 MPa	Reinforcement of haunch
D16	473.6 MPa	661.1 MPa	1.795×10^5 MPa	Main rebar of beam and column
D19	600.4 MPa	796.6 MPa	1.797×10^5 MPa	Main rebar of beam

Table 7. Mechanical properties of concrete

Casting zone		Compressive strength σ_B	Young's modulus of elasticity E*	Split tensile strength σ_t
Precast portion of beam Lower column		55.2 MPa	3.15×10^4 MPa	4.05 MPa
Cast-in-place portion of beam, joint	JNo.1	50.6 MPa	3.04×10^4 MPa	3.88 MPa
	JNo2, 3	33.3 MPa	2.57×10^4 MPa	2.89 MPa
Upper column		48.5 MPa	2.86×10^4 MPa	3.69 MPa

E* : measured at 1/4th of σ_B

Table 8. Experimental results at maximum load

		Left beam		Right beam		Joint			
		Q_{bm}	$Q_{bm}/{}_{cal}Q_{bm}$	Q_{bm}	$Q_{bm}/{}_{cal}Q_{bm}$	Q_{pm}	τ_{pm}/σ_B	$Q_{pm}/{}_{cal}Q_{pm}$	γ_p
JNo.1	+	2.65	1.21	2.61	1.19	17.75	0.32	0.98	5.42
	-	2.46	1.13	2.38	1.08	16.41	0.30	0.92	7.87
JNo.2	+	2.59	1.18	2.63	1.20	17.72	0.48	1.32	10.54
	-	2.46	1.12	2.24	1.02	15.97	0.44	1.22	9.81
JNo.3	+	2.81	1.07	2.87	1.09	19.29	0.46	1.26	15.62
	-	2.84	1.08	2.55	0.97	18.29	0.44	1.22	16.64

Qbm: Maximum strength of beam [kN], Qpm: Maximum strength of joint [kN], γ_p: Shear deformation angle in joint panel [$\times 10^{-3}$rad.], calQbm = $(0.9 \Sigma a_t \cdot \sigma_y \cdot d_b)/\ell$ (Approximate equation of AIJ), a_t: Area of main rebar, σ_y: Strength of main rebar, d_b: Effective depth of bream, ℓ: Beam length, calQpm $=(1.88 \cdot \sigma_B{}^{0.718} \cdot 0.0980665^{0.282}) \cdot (Bc+Bb)/2 \cdot j_c$ (Teraoka's equation), σ_B: Concrete strength of joint, Bc: Column width, Bb: Beam width, $j_c = 7/8 \times d_c$, d_c: Effective depth of column.

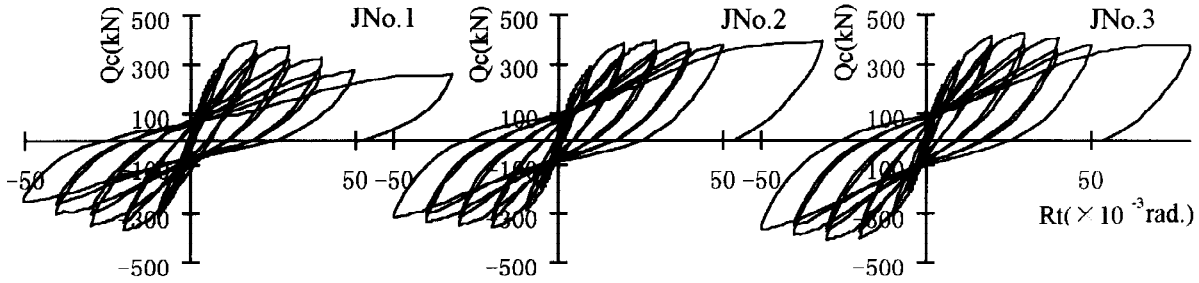

Fig. 6. Hysteresis loops of shear strength of column (Qc) - story deformation angle (Rt)

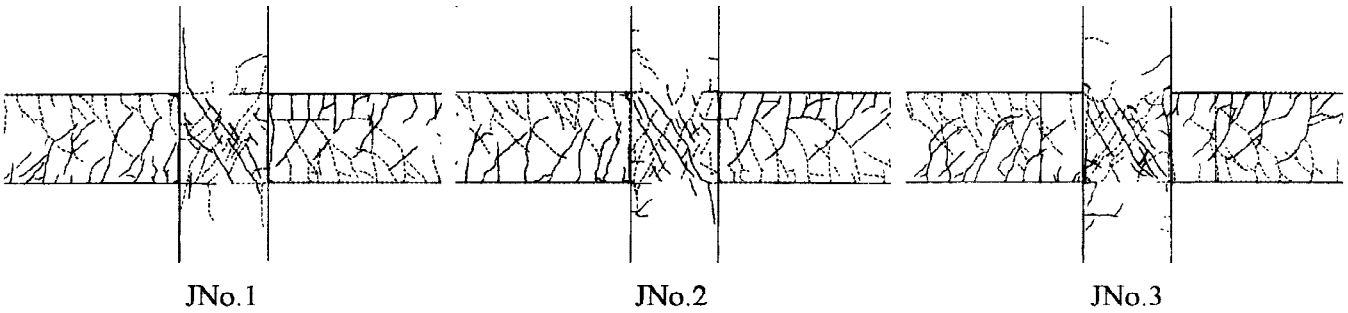

Fig. 7. Cracking patterns around joint (at Rt = 20×10^{-3}rad.)

JNo.2 and 3 at beam yielding is considered to be the shear stress level at the joint failure. The failure of joint panels occurs when the diagonal compressive force on the panel reaches its critical value ; however, reinforcing the joint panel delays the attainment of critical compressive force. Therefore, in specimens JNo.2 and 3, an anchor plate was attached to the tension side of the longitudinal beam reinforcement within the joint panel to secure the truss reaction force at the joint panel corner, and that force was transferred to the member using circular spiral transverse reinforcement. Furthermore, for specimen JNo.3, by combining horizontal haunches and additional longitudinal reinforcement at both ends of the beam, effective volume was increased and hinging of the longitudinal beam reinforcement inside the joint panel was prevented.

Experimental Results

Table 8 tabulates the experimental results at maximum load. Fig. 6 shows the hysteresis loops of shear strength of column (Qc) versus Rt and Fig. 7 shows the cracking patterns around joint at story deformation angle Rt=20×10^{-3} *rad.*

Failure Course and Restoring Force Characteristics The specimen JNo.1, with a joint of Fc=59MPa concrete in joint, suffered beam yielding at Rt =10×10^{-3} *rad* and attained maximum strength at Rt =20×10^{-3} *rad.* On the other hand, the specimens with joint of Fc=29MPa concrete in joint suffered beam yielding at Rt =15×10^{-3} *rad* (JNo.2) and Rt = 23×10^{-3} *rad* (JNo.3), and both of them attained maximum strength at Rt =30×10^{-3} *rad.* This indicated varying yield stiffnesses for the different types of concrete used in joints. For all specimens, the decrease in strengths after attaining the maximum strengths was gradual. All specimens exhibited shear failure at the joint panel after beam yielding. As shown in Fig. 8, the maximum shear strengths for specimens JNo.1 and 2 were identical, and the shear stress level in specimen JNo.2 at the time of maximum loading was $0.48\sigma_{BP}$ (σ_{BP} : concrete strength of joint panel). The reduction of shear strength after maximum loading was less for specimen JNo.2 than for specimen JNo.1.

Effect of Reinforcing Joint Panel Fig. 9 shows the proportion of induced force in joint by beam main

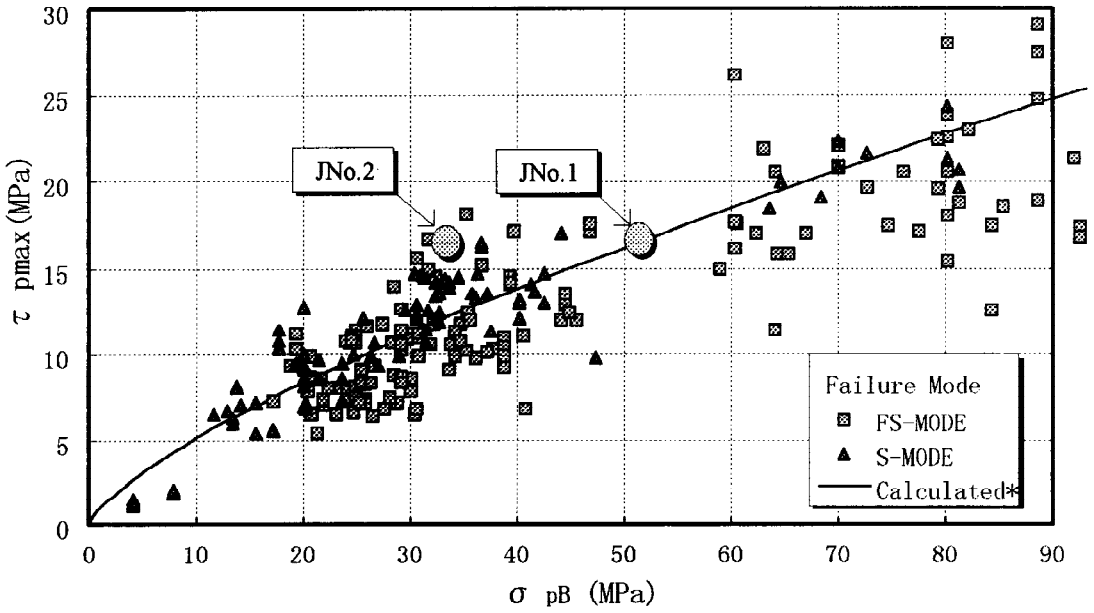

Fig. 8. Ultimate shear strength of joint panel (τ_{pmax}) — compressive strength of concrete (σ_B)

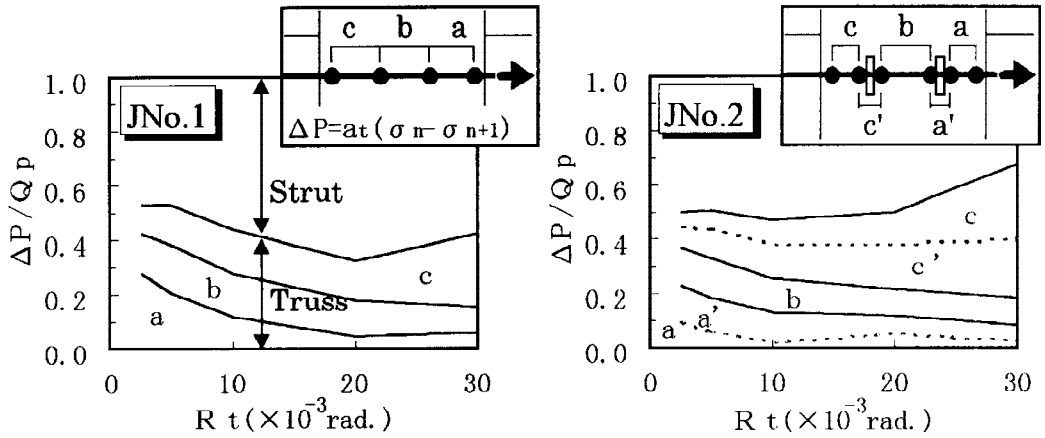

Fig. 9 Proportion of induced force in joint from beam main reinforcement

reinforcement (force of truss mechanism) for specimens JNo.1 and 2. After $Rt=10\times10^{-3}$ *rad*, the proportion of induced force in joint corner 'a' and the force of truss mechanism in specimen JNo.2 were greater than those in JNo.1. At the maximum strength at $Rt=30\times10^{-3}$ *rad*, the force of strut mechanism in JNo.2 was half the force in JNo.1. The effect of reinforcing the joint panel section was greater than the degree of reduction in concrete strength.

CONCLUSION

The following major findings were obtained from the experiments:

(1) When the concrete strengths of the cast-in-place portion (upper part of beam) and the precast portion were different, shear strength of the beam can be estimated by using average strength in terms of sectional areas, in the same way as the estimation of conventional uniform-strength concrete.

(2) By using the additional arrangement of anchorage and transverse reinforcement in joint panels, ductility and shear bearing capacity are much improved over normal design levels.

REFERENCES

Architectural Institute of Japan (1988). Design Guidelines for Earthquake Resistant Reinforced Concrete Buildings Based on Ultimate Strength Concept (Draft).

Hayashi, K., Hayashi, S., Mikame, A. and Teraoka, M. (1994). Study on Mechanical Properties of Precast R/C Beams Using Two Kinds of Concrete. Summaries of Technical Papers of Annual Meeting, Structure II, 979-980, Architectural Institute of Japan.

Hayashi, K., Hayashi, S., Mikame, Satoh, T. (1995). Experimental Study on Reinforcement of R/C Beam-Column Joint Panels. Summaries of Technical Papers of Annual Meeting, Structure II, 63-64, Architectural Institute of Japan.

Teraoka, M., Kanoh, Y., Tanaka, K. and Hayashi, K. (1990). Experimental Studies on Interior Beam-Column Joints Using High-strength Concrete. Proceedings of Japan Concrete Institute, 12-2, 633-638.